

# Quantum synchronization through the interference blockade

Tobias Kehrer, Tobias Nadolny, and Christoph Bruder

Department of Physics, University of Basel, Klingelbergstrasse 82, CH-4056 Basel, Switzerland

(Dated: October 8, 2024)

Synchronization manifests itself in oscillators adjusting their frequencies and phases with respect to an external signal or another oscillator. In the quantum case, new features appear such as destructive interferences that can result in the suppression of phase locking. A three-level (spin-1) oscillator with equal gain and damping rates and subject to an external drive does not exhibit any 1:1 phase locking but 2:1 phase locking, i.e., its phase distribution features two maxima. This bistable locking at two opposite phases is a signature of the quantum interference synchronization blockade. An analogous behavior was found for two identical coupled spin-1 oscillators. In this work, we consider two coupled spin-1 oscillators and a drive applied to the first spin. This leads to two interference blockades between the drive and the first spin as well as between both spins. Although both interference blockades persist for strong drive and coupling strengths, remarkably, the undriven spin does show a 1:1 phase locking to the external drive. The magnitude of the locking is proportional to the drive strength if the drive strength is small. In other words, the undriven oscillator synchronizes to the external drive through both interference blockades while the blockades persist. For a chain of three coupled spin-1 oscillators, we find synchronization between the first and third spins mediated via the blocked, second spin.

## I. INTRODUCTION

Synchronization is observed in many different domains of the natural and life sciences [1–4]. It occurs in systems of coupled limit-cycle oscillators and is characterized by the adjustment of oscillation frequencies to a common frequency or the emergence of maxima in the phase distributions. Synchronization has been thoroughly studied in the context of classical nonlinear dynamics [5–8].

Recently, there has been a lot of activity in the study of synchronization in quantum systems, e.g., quantum limit-cycle oscillators [9, 10] implemented as quantum harmonic oscillators [11–14] or few-level quantum oscillators [15–17] subject to incoherent gain and damping. Observations of quantum synchronization have been reported in several experimental setups such as cold atoms [18], nuclear spins [19], trapped ions [20], and superconducting qubits [21].

A three-level quantum system in which one of the three states is stabilized by incoherent gain and damping processes has been established as a minimal quantum limit-cycle oscillator. Subject to an external drive, this spin-1 oscillator aligns its phase with the drive signal. The magnitude of this so-called 1:1 phase locking is proportional to the drive strength. If the gain and damping rates are equal, an *interference blockade* emerges leading to a complete suppression of 1:1 phase locking [15]. In this case, the oscillator tends to align its phase in one of two positions: in phase or opposite the phase of the drive. This corresponds to 2:1 phase locking. In this work, we will use the term  $n$ :1 phase locking if the phase distribution of an oscillator exhibits  $n$  maxima corresponding to multistable locking. A similar effect is observed for the synchronization of two identical coupled spins 1, i.e., the absence of 1:1 phase locking and the presence of 2:1 phase locking [22]. Interference blockades [23] are not the only type of blockades that have been studied in systems

of quantum oscillators, for another example see [24].

In this work, we first consider a drive applied to one of two coupled spin-1 oscillators. In the parameter regime of equal gain and damping rates, see Fig. 1(b), both spins are blockaded: there is no 1:1 phase locking of the driven spin to the drive as well as no 1:1 phase locking between both spins. They both align in and out of phase corresponding to 2:1 phase locking. Remarkably, the undriven spin *does* exhibit 1:1 phase locking to the external drive. In other words, the undriven oscillator synchronizes to the external drive *through* both (drive-spin and spin-spin) interference blockades *without* lifting them. The locking strength is linear in the drive strength and of third order in the coupling strength. The second system that we study is a chain of three coupled spin-1 oscillators. An unexpected 1:1 phase locking, in analogy to the two-spin case, is found between the first and last spin, see Fig. 1(c). However, the central spin mediating this locking is itself not 1:1 phase locked to any of the other two spins.

The paper is structured as follows. In Sec. II, we define the Lindblad master equation of our systems and the measure of quantum synchronization we will use. In Sec. III, we study the behavior of two spin-1 oscillators in and outside the interference blockades. In Sec. IV, we analyze a system of three coupled spins 1. We summarize our results and conclude in Sec. V.

## II. QUANTIFYING QUANTUM SYNCHRONIZATION

We consider a model of coupled spin-1 oscillators subject to gain and damping processes. The system is de-

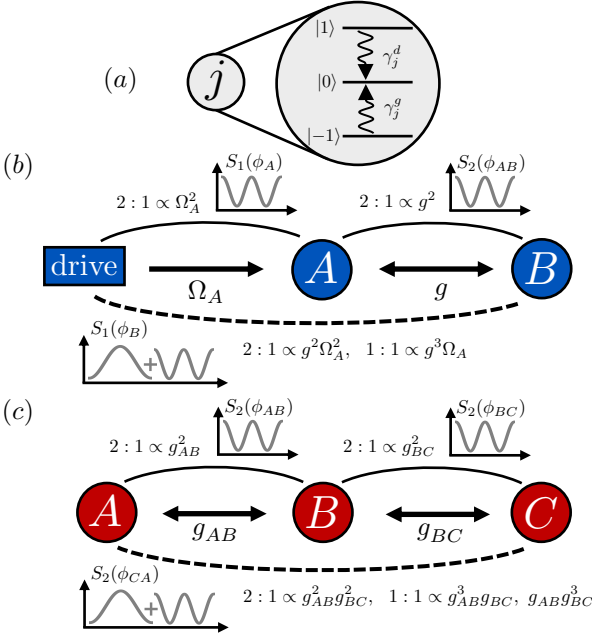


FIG. 1. Schematic of the model. (a) Each minimal quantum limit cycle oscillator labeled  $A$ ,  $B$ , and  $C$  consists of three spin-1 states  $|-1\rangle$ ,  $|0\rangle$ , and  $|1\rangle$ . It is subject to two independent gain and damping processes, with rates  $\gamma_j^g$  and  $\gamma_j^d$ , that drive the population towards state  $|0\rangle$ . (b) Two spins  $A$  and  $B$  are coupled at strength  $g$  as discussed in Sec. III. Spin  $A$  is furthermore driven by an external drive at rate  $\Omega_A$ . (c) Chain of three coupled spins without drive, see Sec. IV. The insets in (b) and (c) qualitatively show the resulting phase locking of the spins. Due to blockades, 1:1 phase locking vanishes. Solid arcs denote second-order effects leading to 2:1 phase locking. Dashed arcs denote fourth-order effects leading to 1:1 and 2:1 phase locking between not directly coupled oscillators.

scribed by the following Lindblad master equation

$$\frac{d}{dt}\rho = \mathcal{L}(\rho) = -i[H, \rho] + \sum_j \mathcal{L}_j(\rho), \quad (1)$$

$$\mathcal{L}_j(\rho) = \frac{\gamma_j^g}{2} \mathcal{D}[S_j^+ S_j^z](\rho) + \frac{\gamma_j^d}{2} \mathcal{D}[S_j^- S_j^z](\rho), \quad (2)$$

where the Hamiltonian  $H$  encodes a coherent drive and spin-spin interactions and will be specified later in Eqs. (8) and (17). Both incoherent processes are combined in the superoperator  $\mathcal{L}_j$  and provide limit-cycle stabilization of the  $j$ th spin, cf. black arrows in Fig. 1(a). The gain and damping rates of the  $j$ th spin are denoted by  $\gamma_j^g$  and  $\gamma_j^d$  and we choose  $S^z = |1\rangle\langle 1| - |-1\rangle\langle -1|$  and  $S^\pm = \sqrt{2}(|\pm 1\rangle\langle 0| + |0\rangle\langle \mp 1|)$ . We use the standard notation  $\mathcal{D}[L](\rho) = L\rho L^\dagger - (L^\dagger L\rho + \rho L^\dagger L)/2$ . The steady state for  $H = 0$  is the product state  $\rho^{(0)} = |0, 0\rangle\langle 0, 0|$ .

A previous work shows that quantum synchronization of a single spin-1 oscillator to an external resonant drive is observed if  $\gamma_j^g \neq \gamma_j^d$  [15]. For two resonant spin-1 oscillators, quantum synchronization occurs if  $\gamma_i^d + \gamma_j^g \neq \gamma_i^g + \gamma_j^d$  [16]. In those works, quantum synchronization is defined

as an effect that is linear in the drive strength or the interaction strength, respectively. If the rate conditions mentioned above are violated, only higher-order synchronization can be observed, i.e., the system is in the quantum interference synchronization blockade.

A variety of measures to quantify the degree of quantum synchronization has been proposed in the literature [11, 15, 25, 26]. For  $N$  spin-1 oscillators, we choose the synchronization measure  $S_N(\vec{\phi})$  defined in [16],

$$S_N(\vec{\phi}) = \left(\frac{3}{4\pi}\right)^N \int_0^\pi d\theta_1 \sin(\theta_1) \dots \times \int_0^\pi d\theta_N \sin(\theta_N) \langle \vec{\theta}, \vec{\phi} | \rho | \vec{\theta}, \vec{\phi} \rangle - \frac{1}{(2\pi)^N}, \quad (3)$$

where

$$|\vec{\theta}, \vec{\phi}\rangle = \bigotimes_j \exp(-i\phi_j S_j^z) \exp(-i\theta_j S_j^y) |1, 1\rangle. \quad (4)$$

This measure is a probability distribution of phases  $\phi_j$  of each oscillator  $j$  that are defined by projections of the density matrix to spin coherent states  $|\vec{\theta}, \vec{\phi}\rangle$ , where  $|S, m_S\rangle = |1, 1\rangle$  is the extremal spin-1 state. Using  $S_N$ , we will calculate probability distributions of relative phase angles as marginals by integrating over global phases, see, e.g., Eq. (5). If the synchronization measure is flat, there is no phase preference, i.e., no synchronization in the system. Maxima of  $S_N$  are related to locking of the oscillator phases. In Appendix A, we show that  $S_N$  can be expressed as expectation values of powers of the spin ladder operators  $S_j^\pm$ , see Eqs. (A9) and (A13). In particular, we find that the phase distributions can be written as

$$S_1(\phi_j) = 2(m_j^{(1)} \cos(\phi_j) + m_j^{(2)} \cos(2\phi_j)), \\ S_2(\phi_{ij}) = \int_0^{2\pi} d\phi S_2(\phi_{ij} + \phi, \phi) \\ = 2(m_{ij}^{(1)} \cos(\phi_{ij}) + m_{ij}^{(2)} \cos(2\phi_{ij})), \quad (5)$$

where  $\phi_{ij} = \phi_i - \phi_j$  is the relative phase of two oscillators  $i$  and  $j$ . Here, we define the moments

$$m_j^{(n)} = \langle (S_j^+)^n \rangle \times \begin{cases} \frac{3}{32} & n = 1, \\ \frac{1}{8\pi} & n = 2, \end{cases} \quad (6)$$

$$m_{ij}^{(n)} = \langle (S_i^+ S_j^-)^n \rangle \times \begin{cases} \frac{9\pi}{512} & n = 1, \\ \frac{1}{32\pi} & n = 2, \end{cases} \quad (7)$$

where the label  $n$  corresponds to  $n$ :1 phase locking and equals the number of maxima in the synchronization measure. Thus, these moments are linked to the Fourier coefficients of the phase distributions and we will use them to quantify synchronization.

### III. TWO SPINS AND A DRIVE

In this section, we consider two coherently coupled spins 1 labeled  $A$  and  $B$ . A resonant coherent drive with strength  $\Omega_A$  acts on spin  $A$ , see Fig. 1(b). The system is described by Eq. (1) with the Hamiltonian in the rotating frame of the drive

$$H = \frac{\Omega_A}{2} S_A^+ + \frac{g}{2} S_A^+ S_B^- + \text{H.c.}, \quad (8)$$

where  $g$  denotes the strength of the coherent coupling. We choose both  $\Omega_A$  and  $g$  to be positive. Note that both spins are assumed to be in resonance with the coherent drive, i.e., the frequency of the external drive is chosen to match exactly the level spacing of the spins.

#### A. In the interference blockade

To study two spins 1 in the quantum interference synchronization blockade, we set the gain and damping rates  $\gamma_A^g = \gamma_A^d = \gamma_B^g = \gamma_B^d = \gamma$  to be equal. We expand the steady state  $\rho_{ss} = \sum_{n=0}^{\infty} \epsilon^n \rho^{(n)}$  of Eq. (1) in powers of  $\epsilon$  for the small Hamiltonian  $\epsilon H$  of Eq. (8). It fulfills

$$\sum_j \mathcal{L}_j(\rho^{(n+1)}) = i[H, \rho^{(n)}]. \quad (9)$$

The synchronization measures up to fourth order in  $\Omega_A$  and  $g$  are

$$S_2(\phi_{AB}) \approx \frac{g^2}{\pi\gamma^2} \cos(2\phi_{AB}) \left( \frac{1}{4} - 2\frac{g^2}{\gamma^2} - \frac{13}{6} \frac{\Omega_A^2}{\gamma^2} \right), \quad (10)$$

$$S_1(\phi_A) \approx \frac{\Omega_A^2}{\pi\gamma^2} \cos(2\phi_A) \left( 1 - 21\frac{g^2}{\gamma^2} - 8\frac{\Omega_A^2}{\gamma^2} \right), \quad (11)$$

$$S_1(\phi_B) \approx \frac{5g^3\Omega_A}{2\gamma^4} \cos(\phi_B) + \frac{3g^2\Omega_A^2}{\pi\gamma^4} \cos(2\phi_B), \quad (12)$$

see Appendix B 2. In this regime of equal gain and damping rates there is no  $\cos(\phi_A)$  and  $\cos(\phi_{AB})$  contribution since both  $m_A^{(1)}$  and  $m_{AB}^{(1)}$  vanish. This is a consequence of the (drive-spin and spin-spin) interference blockades that persist for arbitrary drive and coupling strengths which means there is no 1:1 phase locking of spin  $A$  to the drive and no 1:1 phase locking between spins  $A$  and  $B$ . However, the synchronization measure  $S_1(\phi_B)$  in Eq. (12) features  $\cos(\phi_B)$ . Hence, there is an effective first-order  $\propto \Omega_A$  1:1 phase locking of the undriven spin-1 oscillator to the drive. This 1:1 phase locking is surprising, since spin  $A$  does not distinguish between the phase of the drive and its polar opposite as well as spin  $B$  does not distinguish between in and out of phase locking to spin  $A$ . We refer to this as synchronization through the interference blockade. It is mediated via a third-order  $\propto g^3$  spin-spin interaction as we will explain in more detail below. The second term in Eq. (12) denotes 2:1 phase locking of spin  $B$ .

In the synchronization regime where both  $\Omega_A$  and  $g$  are small compared to  $\gamma$ , the single-maximum 1:1 phase locking of the undriven spin  $B$  to the drive is a small fourth-order effect. However, there is neither 1:1 phase locking of oscillator  $A$  to the drive nor between oscillators  $A$  and  $B$  at any order in  $\Omega_A$  and  $g$ . Both the phase distribution of oscillator  $A$  and the distribution of the relative phase of oscillators  $A$  and  $B$  do not allow to distinguish between the phase angle of the drive and its polar opposite. For any  $\Omega_A$  and  $g$ , only the phase distribution of oscillator  $B$  uniquely reflects the phase of the drive.

This behavior can be traced back to the destructive interference of various coherences that build up. In short, even if spin  $A$  does not show 1:1 phase locking to the drive, the phase of the drive is nevertheless imprinted in the coherences of the full density matrix. Therefore, spin  $B$  can exhibit 1:1 phase locking. While the contributions of the coherences to the synchronization measure of spin  $A$  cancel, they do not cancel for spin  $B$ .

For a detailed explanation, we note that the choice of equal gain and damping rates introduces a symmetry: the master equation Eq. (1) with the Hamiltonian Eq. (8) is invariant under the transformation that effectively exchanges states  $|j\rangle \leftrightarrow |-j\rangle$ ,

$$S_j^\pm \rightarrow Z S_j^\pm Z^\dagger = S_j^\mp, \quad S_j^z \rightarrow Z S_j^z Z^\dagger = -S_j^z, \quad (13)$$

where

$$Z = \exp(i\pi(S_A^x + S_B^x)), \quad S_j^x = (S_j^+ + S_j^-)/2. \quad (14)$$

We find  $\mathcal{L}(Z\rho Z^\dagger) = Z\mathcal{L}(\rho)Z^\dagger$ , which leads to  $\rho_{ss} = Z\rho_{ss}Z^\dagger$ . Using the invariance of the steady state under the symmetry transformation defined in Eq. (13), it follows that  $\langle S_A^+ \rangle = \langle S_A^- \rangle$  and  $\langle S_A^+ S_B^- \rangle = \langle S_A^- S_B^+ \rangle$ , hence  $m_A^{(1)} \propto \langle S_A^+ \rangle$  and  $m_{AB}^{(1)} \propto \langle S_A^+ S_B^- \rangle$  are real. Since the master equation Eq. (1) only consists of real parameters and  $\rho^{(0)}$  is real, even orders  $\rho^{(2n)}$  of the perturbation expansion of the steady state are real and odd orders  $\rho^{(2n+1)}$  are purely imaginary, see Eq. (9). At least up to fourth order in  $\Omega_A$  and  $g$ , both  $m_A^{(1)}$  and  $m_{AB}^{(1)}$  only depend on  $\rho^{(2n+1)}$ , so they must be purely imaginary. Taking into account the symmetry arguments from above they must vanish in the *interference blockade*: while the individual coherences do not vanish, they interfere destructively  $\langle |1\rangle\langle 0| \otimes \mathbb{1} \rangle = -\langle |0\rangle\langle -1| \otimes \mathbb{1} \rangle$  implying  $\langle S_A^+ \rangle = 0$ .

Spin  $A$  can be intuitively interpreted as an effective drive acting on spin  $B$  mediated by the spin-spin coupling. Because of the additional coupling,  $m_B^{(1)}$  depends on  $\rho^{(2n)}$ , and is therefore real. The above arguments that explain the interference blockade of spin  $A$  therefore do not apply, and spin  $B$  is able to synchronize to the external drive. For  $m_B^{(1)}$ , only the terms of order  $g\Omega_A$  interfere destructively but terms of order  $g^3\Omega_A$  survive which we discuss in more detail in Appendix B 1.

In Fig. 2, we plot the individual synchronization measures  $S_1(\phi_A)$  and  $S_1(\phi_B)$  as well as the combined mea-

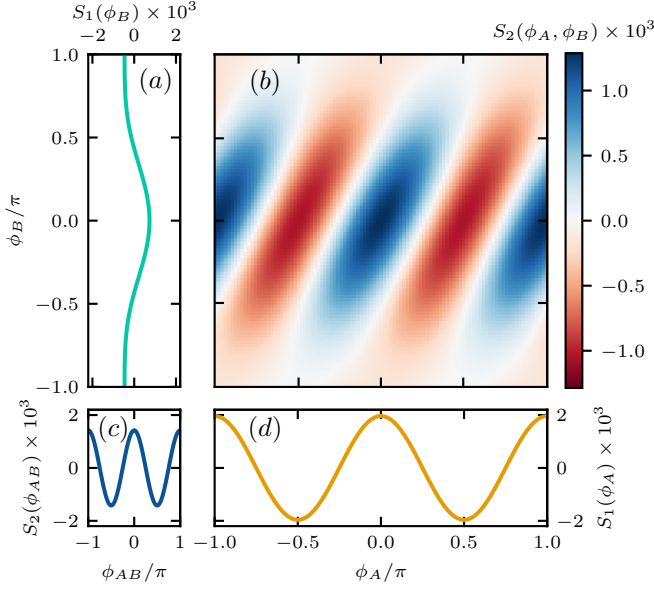


FIG. 2. Synchronization measures  $S_1$  and  $S_2$ , see Eqs. (3) and (5), for  $\Omega_A/\gamma = 0.1$  and  $g/\gamma = 0.15$ . (b) Combined synchronization measure  $S_2(\phi_A, \phi_B)$ . (a),(d) Single synchronization measures  $S_1(\phi_A)$  and  $S_1(\phi_B)$  as marginals of (b). (c) Combined synchronization measure  $S_2(\phi_{AB})$ . Both  $S_2(\phi_{AB})$  and  $S_1(\phi_A)$  exhibit two maxima, whereas  $S_1(\phi_B)$  of the undriven spin in panel (a) is characterized by only one maximum.

asures  $S_2(\phi_A, \phi_B)$  and  $S_2(\phi_{AB} = \phi_A - \phi_B)$ , that are defined in Appendix A, evaluated for the numerically exact steady state of Eq. (1). As expected from Eqs. (10) to (12), both  $S_1(\phi_A)$  and  $S_2(\phi_{AB})$  show two maxima, see Figs. 2(c) and (d). These two distributions imply that spin  $A$  locks with two preferred phases to the drive and spin  $B$  locks with two preferred phases to spin  $A$ . Therefore, one could naively conclude that spin  $B$  also exhibits two maxima in its phase distribution. However, this is not true in general. Figure 2(b) shows that the maxima of the combined quantum synchronization measure lie at  $(\phi_A, \phi_B) \in \{(0, 0), (\pi, 0)\}$ , leading to the single maximum of  $S_1(\phi_B)$ , see Fig. 2(a).

In Fig. 3, we show moments that reflect the synchronization behavior, see Eqs. (6) and (7), for various drive and coupling strengths. As predicted by Eqs. (10) to (12),  $S_1(\phi_B)$  exhibits a first moment, see Fig. 3(c). In contrast, the first moment vanishes for  $S_1(\phi_A)$  and  $S_2(\phi_{AB})$ , see Figs. 3(a) and (b). All synchronization measures show a two-maxima contribution, see Figs. 3(d) to (f). In Fig. 3(g), we plot the ratio of the second and first moment of the undriven spin  $B$  indicating that  $S_1(\phi_B)$  exhibits predominantly two maxima if  $\Omega_A \gg g$  and one maximum if  $\Omega_A \ll g$ . In Fig. 3(h), we show the maximum change in populations between the numerically obtained density matrix  $\rho^{ss}$  and a reference state

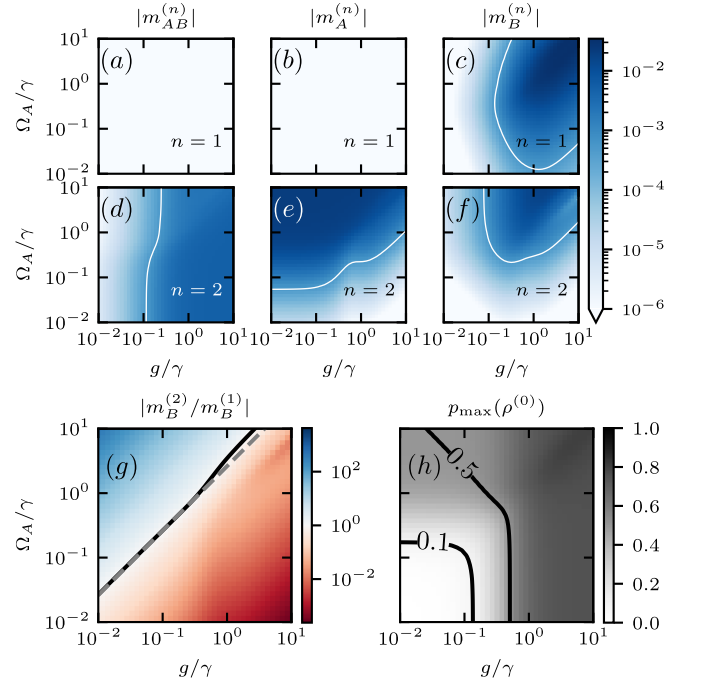


FIG. 3. (a)–(f) First ( $n = 1$ ) and second ( $n = 2$ ) moments indicating one and two maxima in the corresponding synchronization measures. The white curves are contour lines of the moments at  $5 \times 10^{-4}$ . (g) Ratio of the second and first moment of spin  $B$ . The black curve denotes  $|m_B^{(2)}/m_B^{(1)}| = 1$  and the gray dashed lines denote the corresponding theoretical prediction  $\Omega_A = 5\pi g/6$  based on Eq. (12). (h) Maximum change of state populations, see Eq. (15).

$$\rho = \rho^{(0)} = |0, 0\rangle\langle 0, 0| \quad [22]$$

$$p_{\max}(\rho) = \max_n |\rho_{n,n}^{ss} - \rho_{n,n}|. \quad (15)$$

It can be used to identify the regime of synchronization in which the limit-cycle state is only weakly perturbed, i.e.,  $p_{\max} \lesssim 0.1$  which we find to be  $g, \Omega_A \lesssim 0.1\gamma$ . In this region, the fourth-order approximation agrees with the numerical results presented in Figs. 3(a) to (g). Moreover, entanglement measures are small below  $g/\gamma \lesssim 0.1$ , see Appendix C. The relation between quantum synchronization and entanglement has been studied for, e.g., spins [16, 27] and harmonic oscillators [28–30].

Note that if the gain and damping rates are chosen such that only one of either a drive-spin or a spin-spin interference blockade exists, it does not persist up to large drive and coupling strengths. The drive-spin blockade is lifted by the spin-spin interaction and vice versa. Since in these cases  $m_A^{(1)}$  and  $m_{AB}^{(1)}$  are not zero, it is not surprising that also  $m_B^{(1)}$  is not zero. Only when imposing both blockades simultaneously by equal gain and damping rates for all spins, as described in this section, the blockades persist.

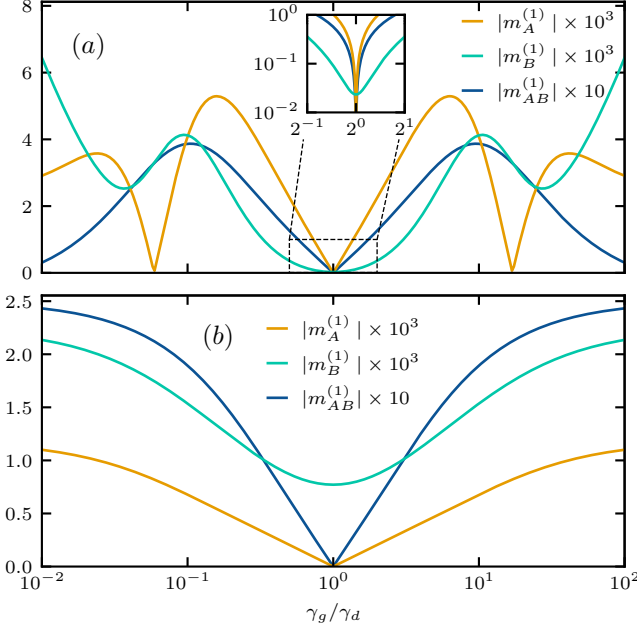


FIG. 4. First moments of the individual and combined synchronization measures for  $\Omega_A/(\gamma_g + \gamma_d) = 10^{-3}$ . (a)  $g/(\gamma_g + \gamma_d) = 0.05$ . The inset highlights the region close to the interference blockade  $\gamma_g = \gamma_d$ . (b)  $g/(\gamma_g + \gamma_d) = 0.5$ .

### B. Outside the interference blockade

In the previous section, synchronization is blocked perfectly. We now discuss the behavior of the two-spin system for inverted gain and damping rates  $\gamma_A^g = \gamma_B^d = \gamma_g$  and  $\gamma_A^d = \gamma_B^g = \gamma_d$  close to the blockade. To this end, we show  $m_A^{(1)}$ ,  $m_B^{(1)}$ , and  $m_{AB}^{(1)}$  in Fig. 4. Whenever  $\gamma_g \neq \gamma_d$ , the symmetry defined by Eq. (13) is broken and the interference blockades disappear such that 1:1 drive-spin and spin-spin phase locking exist. Nevertheless, there is a regime in which  $|m_A^{(1)}| < |m_B^{(1)}|$ . Its width can be estimated by expanding the ratio of the first moments of spin  $A$  and spin  $B$  to first order in  $\gamma_g/\gamma_d - 1$ . This expansion can be used to approximately solve  $|m_A^{(1)}/m_B^{(1)}| = 1$  by

$$\frac{\gamma_g}{\gamma_d} = 1 \pm \frac{20g^3}{3\gamma_d^3} + \mathcal{O}(g^5/\gamma_d^5) \approx 1 \pm \frac{160g^3}{3(\gamma_g + \gamma_d)^3}. \quad (16)$$

The region in which the undriven spin  $B$  exhibits a stronger 1:1 phase locking to the drive than the driven spin  $A$  has an approximate width  $\propto g^3/\gamma_d^3$  in terms of the ratio of gain and damping rates  $\gamma_g/\gamma_d$ .

In addition to the interference blockade, i.e., vanishing  $m_A^{(1)}$  and  $m_{AB}^{(1)}$ , between spin  $A$  and its drive as well as between both spins we find another synchronization blockade that is induced by the coupling. This new and additional blockade appears at roots of  $m_A^{(1)}$  and  $m_{AB}^{(1)}$  for values of  $\gamma_g/\gamma_d$  depending on  $g$ , see Eqs. (B4) to (B6) and Fig. 4(a). In the interference blockade  $\gamma_g = \gamma_d$ , up to first

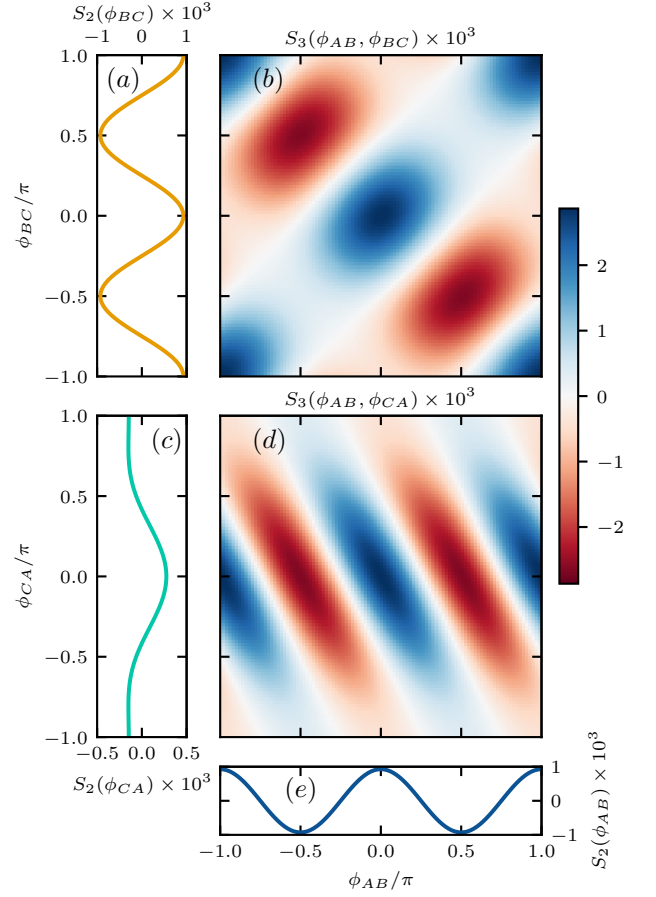


FIG. 5. Synchronization measures  $S_2$  and  $S_3$ , see Eqs. (5), (A16), and (A17), for  $g_{AB}/\gamma = g_{BC}/\gamma = 0.12$ . (b),(d) Combined measures for three coupled spin-1 oscillators. (a),(c),(e) Combined measures for pairs of two spins 1.

order in  $\Omega_A$ , contributions to  $m_{AB}^{(1)}$  originating from both  $|0, 1\rangle\langle 1, 0|$  and  $|-1, 0\rangle\langle 0, -1|$  vanish individually, whereas terms proportional to  $|0, 0\rangle\langle 1, -1|$  and  $|-1, 1\rangle\langle 0, 0|$  cancel. In the coupling-induced blockade, these coherences cancel collectively.

The coupling-induced blockades occur for rather large coupling strengths for which the steady state of the system deviates significantly from  $\rho^{(0)}$ . In the regime  $g \gtrsim \gamma_g + \gamma_d$  one obtains  $p_{\max}(\rho^{(\infty)}) \lesssim 0.1$ , i.e., the steady state is close to  $\rho^{(\infty)}$ .

### IV. THREE UNDRIVEN SPINS

We now consider a system of three undriven coupled spin-1 oscillators labeled  $A$ ,  $B$ , and  $C$ ,

$$H = \frac{g_{AB}}{2} S_A^+ S_B^- + \frac{g_{BC}}{2} S_B^+ S_C^- + \text{H.c.}, \quad (17)$$

where  $g_{AB}$  ( $g_{BC}$ ) is the coupling strength between spins  $A$  and  $B$  ( $B$  and  $C$ ). Similar to Sec. III A, all gain and damping rates are set equal to  $\gamma$ . In Fig. 5, we

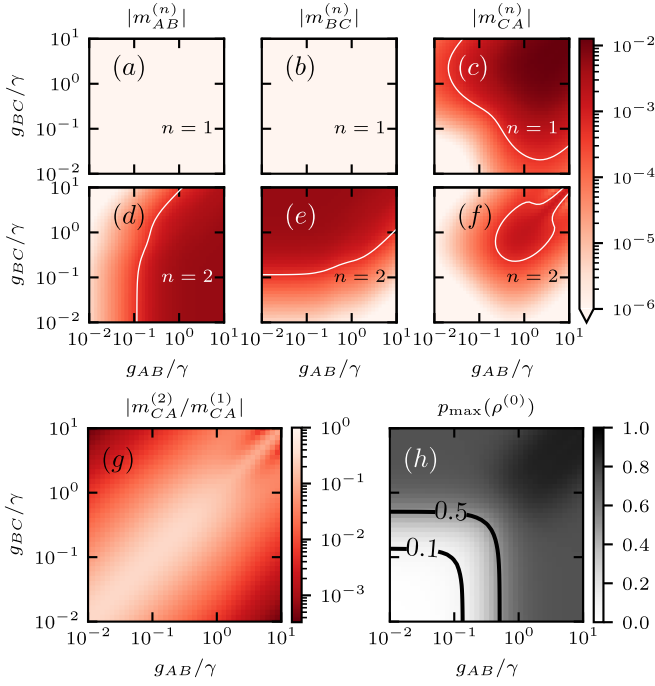


FIG. 6. (a)–(f) First ( $n = 1$ ) and second ( $n = 2$ ) moments indicating one and two maxima in the corresponding synchronization measures. The white curves are contour lines of the moments at  $5 \times 10^{-4}$ . (g) Ratio  $|m_{CA}^{(2)}|/|m_{CA}^{(1)}| < 1$  of the second and first moment of the combined measure of spins  $A$  and  $C$ . (h) Maximum change of a state populations, see Eq. (15).

show both synchronization measures  $S_3(\phi_{AB}, \phi_{BC})$  and  $S_3(\phi_{AB}, \phi_{CA})$ , evaluated for the numerically exact steady state of Eq. (1), for three spins which are probability distributions of the relative phases between the three oscillators, see Eqs. (A16) and (A17). Moreover, we present the synchronization measures  $S_2$  between all three pairs of spins as marginals. As expected,  $S_2(\phi_{AB})$  and  $S_2(\phi_{BC})$  of both pairs of coupled spins exhibit two maxima due to the quantum interference synchronization blockade, see Figs. 5(a) and (e). However, similar to the single-maximum locking of the undriven spin  $B$  in Fig. 2(a), the synchronization measure between the spins  $A$  and  $C$  that are not directly coupled exhibits a single maximum in the phase difference  $\phi_{CA}$ , see Fig. 5(c). This contradicts the naive expectation that if  $S_2(\phi_{AB})$  and  $S_2(\phi_{BC})$  exhibit two maxima,  $S_2(\phi_{CA})$  will also exhibit two maxima. In fact, the synchronization measures  $S_3(\phi_{AB}, \phi_{BC})$  and  $S_3(\phi_{AB}, \phi_{CA})$  exhibit maxima at  $(\phi_{AB}, \phi_{BC}, \phi_{CA}) \in \{(0, 0, 0), (\pi, \pi, 0)\}$  revealing the true locking behavior: the phases of neighboring spins are either aligned or anti-aligned.

In analogy to Fig. 3, we display relevant moments of the three-spin system in Fig. 6. Figures 6(a) and (b) show vanishing 1:1 phase locking between directly coupled spins. In contrast, Fig. 6(c) shows 1:1 phase locking between the spins  $A$  and  $C$  that are not directly coupled. Similar to what was found for the undriven spin  $B$

discussed in Sec. III, the quantum synchronization measure between the uncoupled spins  $A$  and  $C$  exhibits both non-vanishing first and second moments. All synchronization measures exhibit a two-maxima contribution, see Figs. 6(d) to (f). Interestingly, in contrast to the setup of two spin-1 oscillators, Fig. 6(g) shows that the first moment always dominates, i.e.,  $|m_{CA}^{(2)}| < |m_{CA}^{(1)}|$ . In the region  $g_{AB}, g_{BC} \lesssim 0.1\gamma$ , entanglement measures are small, see Fig. 8 in Appendix C. This matches the region of  $p_{\max} \lesssim 0.1$  in Fig. 6(h).

## V. CONCLUSION

We have analyzed setups of two and three coupled spin-1 oscillators in the parameter regime of equal gain and damping rates leading to (spin-spin) quantum interference blockades between all coupled oscillators. In the case of two spins, a drive acting on spin  $A$  leads to a second type of (drive-spin) quantum interference blockade. Both blockades persist for arbitrarily large drive and coupling strengths.

In the two-spin setup, the blockades manifest themselves in vanishing first moments of the quantum synchronization measure of spin  $A$  as well as of the combined synchronization measure of both spins. Spin  $A$  synchronizes with equal probability in and out of phase with the drive with a magnitude proportional to the square of the drive strength  $\Omega_A$ . Similarly, spin  $B$  locks in and out of phase to spin  $A$  with a magnitude proportional to the square of the coupling strength  $g$ . The naive expectation that spin  $B$  will therefore also lock with two preferred phases to the drive fails in general. The undriven spin  $B$  exhibits a 1:1 phase locking to the drive through both blockades without lifting them. The magnitude of this 1:1 phase locking is proportional to  $g^3\Omega_A$  corresponding to a first-order locking to the drive mediated via a third-order spin-spin interaction. Remarkably, the driven spin  $A$  exhibits no 1:1 phase locking. If the parameters are chosen such that only one of either a drive-spin or a spin-spin interference blockade exists, it does not persist up to large drive and coupling strengths. The drive-spin blockade is lifted by the spin-spin interaction and vice versa. Only when imposing both blockades simultaneously by equal gain and damping rates for all spins, the blockades persist.

In a three-spin chain, the combined quantum synchronization measures of both pairs of directly coupled spins exhibit two maxima. However, similar to the two-spin case discussed in the previous paragraph, we observe a 1:1 phase locking behavior between the two not directly coupled spins  $A$  and  $C$ . Analogously, this locking exists without lifting the quantum interference blockades in the other two subsystems  $AB$  and  $BC$ .

Quantum synchronization thus provides a rich set of interesting features. Even for systems whose building blocks are the simplest possible quantum limit-cycle oscillators, unexpected properties arise like the locking of

two not directly coupled spins mediated by an intermediate spin that is itself not locked. An intriguing question for the future is the study of the competition of single-maximum (indirect coupling) and two-maxima locking (direct coupling) in geometrically frustrated configurations of spin-1 oscillators.

### ACKNOWLEDGMENTS

We acknowledge financial support from the Swiss National Science Foundation individual grant (Grant No. 200020 200481). We furthermore acknowledge the use of QUTIP [31].

### Appendix A: Quantum Synchronization Measures

We use the measure of quantum synchronization for single spin- $S$  oscillators introduced in [15],

$$S_1(\phi) = \int_0^\pi d\theta \sin(\theta) Q(\theta, \phi, \rho) - \frac{1}{2\pi}, \quad (\text{A1})$$

where

$$Q(\theta, \phi, \rho) = \frac{2S+1}{4\pi} \langle \theta, \phi | \rho | \theta, \phi \rangle \quad (\text{A2})$$

is the Husimi  $Q$  function of  $\rho$  with respect to spin coherent states

$$|\theta, \phi\rangle = \exp(-i\phi S^z) \exp(-i\theta S^y) |S, S\rangle, \quad (\text{A3})$$

and  $|S, m_S = S\rangle$  is the extremal spin- $S$  state. Using the Wigner  $D$  matrix [32], we can express Eq. (A2) as

$$Q(\theta, \phi, \rho) = \frac{2S+1}{4\pi} \sum_{n,m} e^{i(n-m)\phi} d_{n,S}^S(\theta) d_{m,S}^S(\theta) \rho_{n,m}, \quad (\text{A4})$$

where

$$d_{n,S}^S(\theta) = \sqrt{\frac{(2S)!}{(S+n)!(S-n)!}} \cos\left(\frac{\theta}{2}\right)^{S+n} \sin\left(\frac{\theta}{2}\right)^{S-n}. \quad (\text{A5})$$

The integration over  $\theta$  in Eq. (A1) can be mapped to Eq. (3.621.5) of [33], leading to

$$S_1(\phi) = \text{Tr} [c^S(\phi) \rho] - \frac{1}{2\pi} = \langle c^S(\phi) \rangle - \frac{1}{2\pi}, \quad (\text{A6})$$

where [34]

$$\begin{aligned} c_{n,m}^S(\phi) &= e^{i(n-m)\phi} \frac{2S+1}{4\pi} \int_0^\pi d\theta \sin(\theta) d_{n,S}^S(\theta) d_{m,S}^S(\theta) \\ &= \frac{e^{i(n-m)\phi}}{2\pi} \frac{\Gamma(1+S+\frac{n+m}{2}) \Gamma(1+S-\frac{n+m}{2})}{\sqrt{(S+n)!(S-n)!(S+m)!(S-m)!}} \end{aligned} \quad (\text{A7})$$

are the components of the operator  $c^S(\phi)$ . For spin-1/2 and spin-1 oscillators, we find explicit expressions for  $c^S(\phi)$ ,

$$c^{\frac{1}{2}}(\phi) = \frac{\mathbb{1}}{2\pi} + \frac{1}{8} (e^{i\phi} S^+ + e^{-i\phi} S^-), \quad (\text{A8})$$

$$c^1(\phi) = \frac{\mathbb{1}}{2\pi} + \left( \frac{3e^{i\phi}}{32} S^+ + \frac{e^{i2\phi}}{8\pi} (S^+)^2 + \text{H.c.} \right). \quad (\text{A9})$$

For larger spins, the expression of  $c^S$  becomes more complex, e.g.,  $c^{\frac{3}{2}}(\phi)$  features terms of the form  $(S^+)^2 S^-$  and  $S^- (S^+)^2$ .

The definition of the synchronization measure Eq. (A1) can be generalized to systems consisting of  $N$  spin- $S$  oscillators by considering tensor products of spin coherent states, see [16],

$$\begin{aligned} S_N(\vec{\phi}) &= \int_0^\pi d\theta_1 \sin(\theta_1) \dots \\ &\times \int_0^\pi d\theta_N \sin(\theta_N) Q(\vec{\theta}, \vec{\phi}, \rho) - \frac{1}{(2\pi)^N}, \end{aligned} \quad (\text{A10})$$

where

$$Q(\vec{\theta}, \vec{\phi}, \rho) = \left( \frac{2S+1}{4\pi} \right)^N \langle \vec{\theta}, \vec{\phi} | \rho | \vec{\theta}, \vec{\phi} \rangle, \quad (\text{A11})$$

$$|\vec{\theta}, \vec{\phi}\rangle = \bigotimes_{j=1}^N \exp(-i\phi_j S^z) \exp(-i\theta_j S^y) |S, S\rangle. \quad (\text{A12})$$

Due to this tensor-product structure, we can express Eq. (A10) as

$$S_N(\vec{\phi}) = \left\langle \bigotimes_{j=1}^N c^S(\phi_j) \right\rangle - \frac{1}{(2\pi)^N}. \quad (\text{A13})$$

In this work, we are interested in up to three spin-1 oscillators. Combining Eqs. (A9) and (A13), for a single spin 1, we obtain

$$S_1(\phi) = \left\langle \frac{3}{32} e^{i\phi} S^+ + \frac{e^{i2\phi}}{8\pi} (S^+)^2 + \text{H.c.} \right\rangle, \quad (\text{A14})$$

and for a system consisting of two spins 1,

$$\begin{aligned} S_2(\phi_{AB}) &= \int_0^{2\pi} d\phi_B S_2(\phi_{AB} + \phi_B, \phi_B) \\ &= \left\langle \frac{9\pi}{512} e^{i\phi_{AB}} S_A^+ S_B^- + \frac{e^{i2\phi_{AB}}}{32\pi} (S_A^+ S_B^-)^2 + \text{H.c.} \right\rangle. \end{aligned} \quad (\text{A15})$$

The structure of Eq. (A9) allows us to express the Fourier transform of  $S_N$  as expectation values of powers of the spin-1 ladder operators  $S_j^\pm$ . Note that the coefficients of

Eq. (A15)  $9\pi/512 = 2\pi(3/32)^2$  and  $1/32\pi = 2\pi/(8\pi)^2$  are related to squares of the coefficients of Eq. (A14), where the additional factor of  $2\pi$  arises from the integration over  $\phi_B$ . Similarly, for three spins, we obtain

$$S_3(\phi_{AB}, \phi_{BC}) = \int_0^{2\pi} d\phi_B S_3(\phi_{AB} + \phi_B, \phi_B, \phi_B - \phi_{BC}), \quad (\text{A16})$$

$$S_3(\phi_{AB}, \phi_{CA}) = \int_0^{2\pi} d\phi_A S_3(\phi_A, \phi_A - \phi_{AB}, \phi_{CA} + \phi_A). \quad (\text{A17})$$

## Appendix B: Strong Drive and/or Coupling

For vanishing drive  $\Omega_A = 0$  or vanishing coupling  $g = 0$ , we can solve the system of two spin-1 oscillators for arbitrary gain and damping rates analytically.

### 1. Inverted Gain and Damping Rates

In the case of inverted gain and damping rates  $\gamma_A^g = \gamma_B^d = \gamma_g$  and  $\gamma_A^d = \gamma_B^g = \gamma_d$  both  $m_A^{(1)}$  and  $m_{AB}^{(1)}$  do not vanish. Solving the system for  $\Omega_A = 0$  and adding a drive that acts on spin  $A$  as a small perturbation leads to the following leading-order contributions in  $\Omega_A/\gamma$ ,

$$m_A^{(1)} = i \frac{3\Omega_A}{16} \frac{\gamma_g - \gamma_d}{\gamma_g \gamma_d} \left( 1 - 4g^2 \frac{(\gamma_g^2 + 4\gamma_g \gamma_d + \gamma_d^2)}{\gamma_g^2 \gamma_d^2} + \mathcal{O}\left(\frac{g^4}{\gamma_d^4}\right) \right), \quad (\text{B1})$$

$$m_B^{(1)} = \frac{3\Omega_{Ag}}{8\gamma_g \gamma_d} \left( \frac{(\gamma_d - \gamma_g)^2}{\gamma_g \gamma_d} + g^2 \frac{320\gamma_g^3 \gamma_d^3 + 23(\gamma_g^4 \gamma_d^2 + \gamma_g^2 \gamma_d^4) - 32(\gamma_g^6 + \gamma_d^6) - 106(\gamma_g^5 \gamma_d + \gamma_g \gamma_d^5)}{3\gamma_g^3 \gamma_d^3 (2\gamma_g + \gamma_d)(\gamma_g + 2\gamma_d)} + \mathcal{O}\left(\frac{g^4}{\gamma_d^4}\right) \right) \quad (\text{B2})$$

$$\begin{aligned} m_{AB}^{(1)} &= i \frac{9\pi g}{256} \frac{\overbrace{2(\gamma_d - \gamma_g)g^2 \gamma_g \gamma_d}^{\text{from } |0,1\rangle\langle 1,0|} + \overbrace{2(\gamma_d - \gamma_g)g^2 \gamma_g \gamma_d}^{\text{from } |-1,0\rangle\langle 0,-1|} + (4g^2 + \gamma_g \gamma_d) \left( \overbrace{(g^2 + \gamma_g^2)\gamma_d}^{\text{from } |0,0\rangle\langle 1,-1|} - \overbrace{(g^2 + \gamma_d^2)\gamma_g}^{\text{from } |-1,1\rangle\langle 0,0|} \right)}{32g^6 + \gamma_g^3 \gamma_d^3 + 4g^4(2\gamma_g^2 + 7\gamma_g \gamma_d + 2\gamma_d^2) + g^2 \gamma_g \gamma_d (4\gamma_g^2 + 5\gamma_g \gamma_d + 4\gamma_d^2)} \\ &= i \frac{9\pi g}{256} \frac{(\gamma_d - \gamma_g)(4g^4 + g^2 \gamma_g \gamma_d - \gamma_g^2 \gamma_d^2)}{32g^6 + \gamma_g^3 \gamma_d^3 + 4g^4(2\gamma_g^2 + 7\gamma_g \gamma_d + 2\gamma_d^2) + g^2 \gamma_g \gamma_d (4\gamma_g^2 + 5\gamma_g \gamma_d + 4\gamma_d^2)}. \end{aligned} \quad (\text{B3})$$

The known interference blockades for  $m_A^{(1)}$ ,  $m_{AB}^{(1)}$ , and the leading order of  $m_B^{(1)}$  arise for  $\gamma_g = \gamma_d$  [15, 16]. The contributions of the coherences  $|i, j\rangle\langle k, l|$  to  $m_{AB}^{(1)}$  are highlighted in the first line of Eq. (B3). Terms originating from both  $|0, 1\rangle\langle 1, 0|$  and  $|-1, 0\rangle\langle 0, -1|$  vanish individually, whereas terms proportional to  $|0, 0\rangle\langle 1, -1|$  and  $|-1, 1\rangle\langle 0, 0|$  cancel in this interference blockade. For  $m_B^{(1)}$ , the coherences  $|0, -1\rangle\langle 0, 0|$  and  $|0, 0\rangle\langle 0, 1|$  cancel with the coherences  $|-1, 0\rangle\langle -1, 1|$  and  $|1, -1\rangle\langle 1, 0|$ . Note that contributions to  $m_B^{(1)}$  of order  $g^3 \Omega_A$  and higher do not vanish for equal gain and damping rates as we will see in the next section. There, additional coherences  $|1, 0\rangle\langle 1, 1|$  and  $|-1, -1\rangle\langle -1, 0|$  appear. The remaining terms of  $m_B^{(1)}$  in the interference blockade can be interpreted as first-order synchronization  $\propto \Omega_A$  of the undriven spin  $B$  to the drive that acts on spin  $A$  mediated via a third-order spin-spin interaction  $\propto g^3$ . We also recognize that the absolute values of the first moments  $m_A^{(1)}$ ,  $m_B^{(1)}$ , and  $m_{AB}^{(1)}$  are invariant under the exchange of the gain and damping rates.

A new coupling-induced blockade, in which contributing coherences cancel collectively, arises for certain relations between the coupling strength  $g$  and the gain and

damping rates. The solution of  $m_{AB}^{(1)} = 0$  can be obtained analytically as

$$\frac{\gamma_g}{\gamma_d} = \frac{1}{2}(1 + \sqrt{17}) \frac{g^2}{\gamma_d^2} \approx \frac{1}{2}(1 + \sqrt{17}) \frac{g^2}{(\gamma_g + \gamma_d)^2}, \quad (\text{B4})$$

where the approximation holds for  $g, \gamma_g \ll \gamma_d$ . The solution of  $m_A^{(1)} = 0$  is obtained approximatively for (a) large  $\gamma_g \gg \gamma_d$  and for (b) both large  $\gamma_g, g \gg \gamma_d$

$$\frac{g}{\gamma_d} \stackrel{\text{(a)}}{\approx} \frac{1}{2} \sqrt{1 + \sqrt{10}}, \quad \frac{\gamma_g}{\gamma_d} \approx \frac{2}{\sqrt{1 + \sqrt{10}}} \frac{g}{\gamma_d}, \quad (\text{B5})$$

$$\frac{g}{\gamma_d} \stackrel{\text{(b)}}{\approx} 1.323, \quad \frac{\gamma_g}{\gamma_d} \approx 0.7561 \frac{g}{\gamma_d}. \quad (\text{B6})$$

### 2. Equal Gain and Damping Rates

In the case of equal gain and damping rates  $\gamma_A^{g/d} = \gamma_B^{g/d} = \gamma$ , for  $\Omega_A = 0$ , we obtain

$$\begin{aligned} \rho^{\text{ss}} &= \left( 1 - \frac{8g^2}{8g^2 + \gamma^2} \right) \rho^{(0)} + \frac{32g^2}{32g^2 + 4\gamma^2} \rho^{(\infty)} \\ &\quad - i \frac{g\gamma}{16g^2 + 2\gamma^2} [S_A^+ S_B^- + \text{H.c.}, \rho^{(0)}], \end{aligned} \quad (\text{B7})$$

where

$$\begin{aligned} \rho^{(\infty)} &= \frac{1}{8} \sum_{J=1,2} \sum_{M=-1,1} |J, M\rangle_c \langle J, M|_c \\ &+ \frac{1}{4} \sum_{J=0,2} |J, 0\rangle_c \langle J, 0|_c = \frac{1}{32} (S_A^+ S_B^- + S_A^- S_B^+)^2 \end{aligned} \quad (\text{B8})$$

is the state in the limit  $g \gg \gamma$  and is diagonal in the combined spin basis  $|J, M\rangle_c$  of two spins 1. We now add a drive that acts on spin  $A$  as a small perturbation. This results in the following leading-order contributions in  $\Omega_A/\gamma$  to the moments of the synchronization measure of the undriven spin  $B$

$$\begin{aligned} m_B^{(1)} &\approx \frac{3}{4} \frac{g^3 \Omega_A (64g^4 + 348g^2\gamma^2 + 135\gamma^4)}{(8g^2 + \gamma^2)(4g^2 + 9\gamma^2)(16g^4 + 72g^2\gamma^2 + 9\gamma^4)} \\ &\stackrel{g \gg \gamma}{\approx} \frac{3\Omega_A}{32g} \\ &\stackrel{g \ll \gamma}{\approx} \frac{5g^3 \Omega_A}{4\gamma^4}, \quad (\text{B9}) \\ m_B^{(2)} &\approx \frac{3}{2\pi} \frac{g^2 \Omega_A^2}{(g^2 + \gamma^2)(4g^2 + \gamma^2)} \\ &\times \frac{96g^8 + 656g^6\gamma^2 + 518g^4\gamma^4 + 108g^2\gamma^6 + 81\gamma^8}{(8g^2 + \gamma^2)(4g^2 + 9\gamma^2)(16g^4 + 72g^2\gamma^2 + 9\gamma^4)} \\ &\stackrel{g \gg \gamma}{\approx} \frac{9\Omega_A^2}{128\pi g^2} \\ &\stackrel{g \ll \gamma}{\approx} \frac{3g^2 \Omega_A^2}{2\pi\gamma^4}. \quad (\text{B10}) \end{aligned}$$

The undriven spin  $B$  exhibits a 1:1 phase locking to the drive with a magnitude that to leading order is linear in  $\Omega_A/\gamma$ . The second moment of the combined synchronization measure for both spins is up to second order in  $\Omega_A/\gamma$  proportional to

$$\begin{aligned} m_{AB}^{(2)} &\approx \frac{1}{8\pi} \frac{g^2}{8g^2 + \gamma^2} \\ &\times \left( 1 - \frac{\Omega_A^2 (848g^6 + 4600g^4\gamma^2 + 1905g^2\gamma^4 + 702\gamma^6)}{(8g^2 + \gamma^2)(4g^2 + 9\gamma^2)(16g^4 + 72g^2\gamma^2 + 9\gamma^4)} \right) \\ &\stackrel{g \gg \gamma}{\approx} \frac{1}{64\pi} - \frac{53\Omega_A^2 + 4\gamma^2}{2048\pi g^2} \\ &\stackrel{g \ll \gamma}{\approx} \frac{g^2}{8\pi\gamma^2} \left( 1 - \frac{26\Omega_A^2 + 24g^2}{3\gamma^4} \right). \quad (\text{B11}) \end{aligned}$$

Analogously, for a vanishing spin-spin interaction strength  $g = 0$ , we obtain

$$\begin{aligned} \rho^{\text{ss}} &= \left( 1 - \frac{8\Omega_A^2}{8\Omega_A^2 + \gamma^2} \right) \rho^{(0)} - \frac{\Omega_A^2}{8\Omega_A^2 + \gamma^2} [S_A^+ + S_A^-, \rho^{(0)}]^2 \\ &- i \frac{\Omega_A \gamma}{8\Omega_A^2 + \gamma^2} [S_A^+ + S_A^-, \rho^{(0)}], \quad (\text{B12}) \end{aligned}$$

leading to the following contribution to the second moment of the synchronization measure of the driven spin

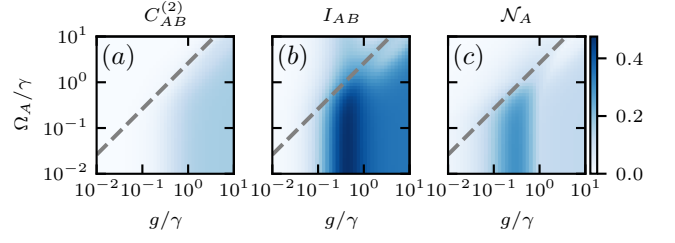


FIG. 7. (a) Correlations  $C_{AB}^{(2)}$  related to Figs. 3(d) to (f). (b) Quantum mutual information of spin  $A$  and  $B$ . (c) Negativity of spin  $A$ . All measures are evaluated for the steady state of the Lindblad master equation. The gray dashed line denotes the theoretical prediction  $\Omega_A = 5\pi g/6$  of  $|m_B^{(2)}/m_B^{(1)}| = 1$ , cf. Fig. 3.

$A$  up to second order in  $g/\gamma$ ,

$$\begin{aligned} m_A^{(2)} &\approx \frac{1}{2\pi} \frac{\Omega_A^2}{8\Omega_A^2 + \gamma^2} \\ &\times \left( 1 - \frac{g^2 (448\Omega_A^4 + 456\Omega_A^2\gamma^2 + 189\gamma^2)}{(8\Omega_A^2 + \gamma^2)(16\Omega_A^4 + 30\Omega_A^2\gamma^2 + 9\gamma^4)} \right) \\ &\stackrel{\Omega_A \gg \gamma}{\approx} \frac{1}{16\pi} - \frac{28g^2 + \gamma^2}{128\pi\Omega_A^2} \\ &\stackrel{\Omega_A \ll \gamma}{\approx} \frac{\Omega_A^2}{2\pi\gamma^2} \left( 1 - \frac{21g^2 + 8\Omega_A^2}{\gamma^4} \right). \quad (\text{B13}) \end{aligned}$$

Note that for equal gain and damping rates, the first moment  $m_A^{(1)}$  of the synchronization measure of the single spin  $A$  and  $m_{AB}^{(1)}$  of the combined synchronization measure vanish, i.e., the system is in the quantum interference blockade.

### Appendix C: Entanglement Measures

In this appendix, we compute correlations

$$C_{ij}^{(n)} = \frac{\text{COV}_{ij}^{(n)}}{\sqrt{\text{COV}_{ii}^{(n)} \text{COV}_{jj}^{(n)}}}, \quad (\text{C1})$$

$$\text{COV}_{ij}^{(n)} = \langle (S_i^- S_j^+)^n \rangle - \langle (S_i^-)^n \rangle \langle (S_j^+)^n \rangle, \quad (\text{C2})$$

and entanglement measures

$$I_{ij} = S(\rho_i : \rho_j) = S(\rho_i) + S(\rho_j) - S(\rho_{ij}), \quad (\text{C3})$$

$$\mathcal{N}_j(\rho) = \frac{\|\rho^{T_j}\|_1 - 1}{2} = \sum_k \frac{|\lambda_k| - \lambda_k}{2}, \quad (\text{C4})$$

where  $I_{ij}$  is the quantum mutual information,  $S(\rho)$  is the von Neumann entropy, and  $\mathcal{N}_j$  is the negativity. The eigenvalues of  $\rho^{T_j}$  are denoted by  $\lambda_k$ , where  $T_j$  indicates the partial transpose that only acts on subsystem  $j$ . Note that in a two-partite system,  $\rho^{T_A}$  and  $\rho^{T_B} = (\rho^{T_A})^T$  have the same eigenvalues and therefore  $\mathcal{N}_A = \mathcal{N}_B$ . For quantum systems of dimensions larger than  $2 \times 3$ , a necessary condition of separability is zero negativity [35, 36].

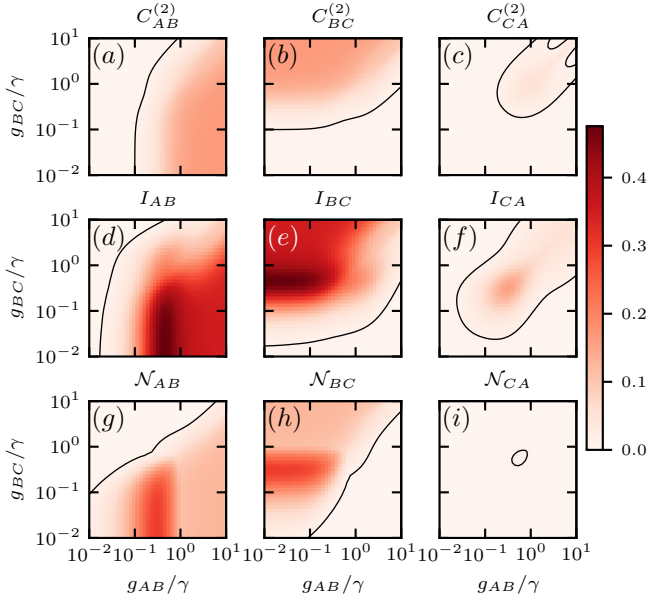


FIG. 8. (a)–(c) Correlations related to Figs. 6(d) to (f). (d)–(f) Quantum mutual information of pairs of spins. (g)–(i) Negativity of pairs of spins. The black curves are contour lines at 0.01.

Therefore,  $\mathcal{N}_j > 0$  implies entanglement. For mixed states, both entanglement and classical correlations contribute to the quantum mutual information  $I_{ij}$ .

We want to highlight the following features of correlations between both spins in the two-spin setup. In Fig. 7, both  $I_{AB}$  and  $\mathcal{N}_A$  exhibit a local maximum between  $0.1\gamma < g < \gamma$  and below the gray dashed line that indicates the theoretical prediction  $\Omega_A = 5\pi g/6$  of  $|m_B^{(2)}/m_B^{(1)}| = 1$ . In this region, the first moment  $m_B^{(1)}$  of the synchronization measure of spin  $B$ , indicating 1:1 phase locking, dominates and  $p_{\max}(\rho^{(0)})$  exhibits a strong change. Comparing all three panels of Fig. 7, in this system, the mutual information  $I_{AB}$  appears to be a combination of correlations, e.g.,  $C_{AB}^{(2)}$ , and entanglement.

In Fig. 8, we present the correlations, quantum mutual information, and negativity between pairs of spin-1 oscillators. We define  $\mathcal{N}_{ij}$  as the negativity of spin  $i$  evaluated for the reduced density matrix of the subsystem of spin  $i$  and  $j$ . The correlations, mutual information, and negativity of subsystem  $AB$  ( $BC$ ) exhibit similar qualitative features, e.g., a local maximum between  $0.1\gamma < g_{AB}$  ( $g_{BC}$ )  $< \gamma$ , as in the two-spin case. The measures of subsystem  $CA$  exhibit local maxima at  $0.1\gamma < g_{AB}, g_{BC} < \gamma$ . Here, qualitatively, the measures of the other two subsystems overlap.

- 
- [1] G. H. Goldsztein, A. N. Nadeau, and S. H. Strogatz, Synchronization of clocks and metronomes: A perturbation analysis based on multiple timescales, *Chaos* **31**, 023109 (2021).
  - [2] J. B. Buck, Synchronous rhythmic flashing of fireflies, *The Quarterly Review of Biology* **13**, 301 (1938).
  - [3] S. H. Strogatz, D. M. Abrams, A. McRobie, B. Eckhardt, and E. Ott, Theoretical mechanics: Crowd synchrony on the Millennium Bridge, *Nature (London)* **438**, 43 (2005).
  - [4] Z. Wang, ed., *Cell-Cycle Synchronization*, Methods in Molecular Biology (Humana, New York, 2022).
  - [5] J. A. Acebrón, L. L. Bonilla, C. J. Pérez Vicente, F. Ritort, and R. Spigler, The Kuramoto model: A simple paradigm for synchronization phenomena, *Rev. Mod. Phys.* **77**, 137 (2005).
  - [6] A. Pikovsky, M. Rosenblum, and J. Kurths, *Synchronization: A Universal Concept in Nonlinear Science* (Cambridge University Press, Cambridge, England, 2001).
  - [7] S. H. Strogatz, *Sync: The Emerging Science of Spontaneous Order* (Hyperion, New York, 2003).
  - [8] K. Okuda and Y. Kuramoto, Mutual entrainment between populations of coupled oscillators, *Progress of Theoretical Physics* **86**, 1159 (1991).
  - [9] A. Chia, L. C. Kwek, and C. Noh, Relaxation oscillations and frequency entrainment in quantum mechanics, *Phys. Rev. E* **102**, 042213 (2020).
  - [10] L. Ben Arosh, M. C. Cross, and R. Lifshitz, Quantum limit cycles and the Rayleigh and van der Pol oscillators, *Phys. Rev. Res.* **3**, 013130 (2021).
  - [11] M. Ludwig and F. Marquardt, Quantum many-body dynamics in optomechanical arrays, *Phys. Rev. Lett.* **111**, 073603 (2013).
  - [12] T. E. Lee and H. R. Sadeghpour, Quantum synchronization of quantum van der Pol oscillators with trapped ions, *Phys. Rev. Lett.* **111**, 234101 (2013).
  - [13] S. Walter, A. Nunnenkamp, and C. Bruder, Quantum synchronization of two van der Pol oscillators, *Annalen der Physik* **527**, 131 (2015).
  - [14] C. W. Wächtler and G. Platero, Topological synchronization of quantum van der pol oscillators, *Phys. Rev. Res.* **5**, 023021 (2023).
  - [15] A. Roulet and C. Bruder, Synchronizing the smallest possible system, *Phys. Rev. Lett.* **121**, 053601 (2018).
  - [16] A. Roulet and C. Bruder, Quantum synchronization and entanglement generation, *Phys. Rev. Lett.* **121**, 063601 (2018).
  - [17] A. Parra-López and J. Bergli, Synchronization in two-level quantum systems, *Phys. Rev. A* **101**, 062104 (2020).
  - [18] A. W. Laskar, P. Adhikary, S. Mondal, P. Katiyar, S. Vinjanampathy, and S. Ghosh, Observation of quantum phase synchronization in spin-1 atoms, *Phys. Rev. Lett.* **125**, 013601 (2020).
  - [19] V. R. Krithika, P. Solanki, S. Vinjanampathy, and T. S. Mahesh, Observation of quantum phase synchronization in a nuclear-spin system, *Phys. Rev. A* **105**, 062206 (2022).
  - [20] L. Zhang, Z. Wang, Y. Wang, J. Zhang, Z. Wu, J. Jie, and Y. Lu, Quantum synchronization of a single trapped-ion qubit, *Phys. Rev. Res.* **5**, 033209 (2023).
  - [21] M. Koppenhöfer, C. Bruder, and A. Roulet, Quantum synchronization on the IBM Q system, *Phys. Rev. Res.* **2**, 023026 (2020).

- [22] M. Koppenhöfer and A. Roulet, Optimal synchronization deep in the quantum regime: Resource and fundamental limit, *Phys. Rev. A* **99**, 043804 (2019).
- [23] P. Solanki, F. M. Mehdi, M. Hajdušek, and S. Vinjanampathy, Symmetries and synchronization blockade, *Phys. Rev. A* **108**, 022216 (2023).
- [24] N. Lörch, S. E. Nigg, A. Nunnenkamp, R. P. Tiwari, and C. Bruder, Quantum synchronization blockade: Energy quantization hinders synchronization of identical oscillators, *Phys. Rev. Lett.* **118**, 243602 (2017).
- [25] T. Weiss, A. Kronwald, and F. Marquardt, Noise-induced transitions in optomechanical synchronization, *New Journal of Physics* **18**, 013043 (2016).
- [26] M. R. Hush, W. Li, S. Genway, I. Lesanovsky, and A. D. Armour, Spin correlations as a probe of quantum synchronization in trapped-ion phonon lasers, *Phys. Rev. A* **91**, 061401(R) (2015).
- [27] A. D. Chepelianskii and D. L. Shepelyansky, Quantum synchronization and entanglement of dissipative qubits coupled to a resonator, *Entropy* **26**, 415 (2024).
- [28] A. Mari, A. Farace, N. Didier, V. Giovannetti, and R. Fazio, Measures of quantum synchronization in continuous variable systems, *Phys. Rev. Lett.* **111**, 103605 (2013).
- [29] T. E. Lee, C.-K. Chan, and S. Wang, Entanglement tongue and quantum synchronization of disordered oscillators, *Phys. Rev. E* **89**, 022913 (2014).
- [30] D. Garg, Manju, S. Dasgupta, and A. Biswas, Quantum synchronization and entanglement of indirectly coupled mechanical oscillators in cavity optomechanics: A numerical study, *Physics Letters A* **457**, 128557 (2023).
- [31] J. Johansson, P. Nation, and F. Nori, QuTiP 2: A Python framework for the dynamics of open quantum systems, *Computer Physics Communications* **184**, 1234 (2013).
- [32] E. P. Wigner, *Group theory: And its application to the quantum mechanics of atomic spectra* (Academic Press, New York, 1959).
- [33] I. Gradshteyn and I. Ryzhik, *Table of Integrals, Series, and Products (Eighth Edition)*, edited by D. Zwillinger and V. Moll (Academic Press, Boston, 2015).
- [34] R. Tan, C. Bruder, and M. Koppenhöfer, Half-integer vs. integer effects in quantum synchronization of spin systems, *Quantum* **6**, 885 (2022).
- [35] A. Peres, Separability criterion for density matrices, *Phys. Rev. Lett.* **77**, 1413 (1996).
- [36] M. Horodecki, P. Horodecki, and R. Horodecki, Separability of mixed states: necessary and sufficient conditions, *Physics Letters A* **223**, 1 (1996).